NMR Detection of Structures in the HIV-1 5′-Leader RNA That Regulate Genome Packaging

Kun Lu,[1]*† Xiao Heng,[1]† Lianko Garyu,[1] Sarah Monti,[1] Eric L. Garcia,[2] Siarhei Kharytonchyk,[2] Bilguujin Dorjsuren,[1] Gowry Kulandaivel,[1] Simonne Jones,[1] Atheeth Hiremath,[1] Sai Sachin Divakaruni,[1] Courtney LaCotti,[1] Shawn Barton,[1] Daniel Tummillo,[1] Azra Hosic,[1] Kedy Edme,[1] Sara Albrecht,[1] Alice Telesnitsky,[2]‡ Michael F. Summers[1]‡

The 5′-leader of the HIV-1 genome regulates multiple functions during viral replication via mechanisms that have yet to be established. We developed a nuclear magnetic resonance approach that enabled direct detection of structural elements within the intact leader (712-nucleotide dimer) that are critical for genome packaging. Residues spanning the *gag* start codon (AUG) form a hairpin in the monomeric leader and base pair with residues of the unique-5′ region (U5) in the dimer. U5:AUG formation promotes dimerization by displacing and exposing a dimer-promoting hairpin and enhances binding by the nucleocapsid (NC) protein, which is the cognate domain of the viral Gag polyprotein that directs packaging. Our findings support a packaging mechanism in which translation, dimerization, NC binding, and packaging are regulated by a common RNA structural switch.

The 5′-leader is the most conserved region of the HIV-1 genome and is responsible for regulating multiple activities during viral replication, including RNA encapsidation during virus assembly (*1*, *2*). Like all retroviruses, HIV-1 packages two copies of its genome, enabling strand-transfer–mediated recombination during reverse transcription and promoting genetic evolution under environmental and chemotherapeutic pressure (*3*). Dimeric genomes are trafficked from the cytoplasm to plasma membrane assembly sites by a small number of viral Gag proteins, where additional Gag proteins assemble and budding occurs (*4*–*8*). Dimerization and packaging are mediated by interactions between the nucleocapsid (NC) domains of the viral Gag polyproteins and RNA elements within the 5′-leader of the genome, and there is evidence that these activities and translational control are mechanistically coupled (*7*, *9*–*13*).

Understanding the mechanisms that regulate 5′-leader activities is limited, in part because of incomplete knowledge of the leader structure (*14*). Recombinant leader-containing RNAs have been probed by nucleotide accessibility mapping, mutagenesis, and biochemical approaches, and although there is general consensus that transcriptional activation, primer binding, dimerization, and splicing activities are promoted by discrete hairpin structures [transacting responsive (TAR), primer-binding site (PBS), dimer initiation site (DIS), and splice donor (SD) hairpins, respectively] (Fig. 1) (*10*, *15*–*23*), there is less agreement regarding the structures that regulate packaging (*14*). In particular, residues overlapping the *gag* start codon [G328 to A356 (AUG)] that are critical for genome packaging (*24*) and RNA dimer stability (*25*) have been proposed to form a hairpin (Fig. 1B), to base pair with residues of the upstream unique-5′ element (U5) (Fig. 1C) (*10*), or to adopt other conformations (*14*). (Single-letter abbreviations for the nucleic acids are as follows: A, adenosine; G, guanosine; C, cytosine; U, uridine.) In vivo nucleotide reactivity mapping has supported multiple AUG models, without consensus (*14*, *21*, *22*). Nuclear magnetic resonance (NMR) is potentially well suited to probe RNA structure, but signal degeneracy and relaxation problems have thus far limited applications to relatively small oligonucleotides (typically fewer than 50 residues) (*26*, *27*). Here, we describe an NMR approach that enabled direct detection of structures formed by AUG and other packaging elements within the intact, 230-kD dimeric 5′-leader as well as the identification of conformational changes that regulate dimerization and NC binding and packaging.

A 356-nucleotide HIV-1_{NL4-3} 5′-leader RNA that includes the entire 5′-untranslated region (5′-UTR) and the first 21 residues of *gag* (5′-L) was prepared by means of enzymatic ligation of non-labeled 5′-RNA (residues 1 to 327) and ^{13}C-enriched AUG fragments (residues 328 to 356) (Fig. 1) (*28*). The 5′-leader exists predominantly as a monomer at low ionic strength (Fig. 1D), and under these conditions, the AUG residues of 5′-L gave rise to ^{1}H-^{13}C–correlated heteronuclear multiple-quantum coherence (HMQC) (*28*) NMR spectra similar to those observed for the isolated AUG fragment, which is known to form a hairpin (Fig. 1, E and F) (*29*). NMR line widths of AUG in the intact 5′-leader and the isolated AUG RNA were also similar, indicating that the hairpin is structurally mobile and does not form A-minor–like contacts (*30*).

Substantial changes in the ^{1}H-^{13}C HMQC spectra of AUG-labeled 5′-L were observed upon incubation at physiological ionic strength [physiological ion (PI) buffer: 10 mM Tris-HCl, 140 mM KCl, 10 mM NaCl, 1 mM $MgCl_2$, pH 7.0], which correspond to a reversible equilibrium shift from a predominantly monomeric species to a mixture of monomeric and dimeric species [dimer dissociation constant (K_d) = 0.9 ± 0.1 μM] (Fig. 1, G and H). Signals of the AUG hairpin in 5′-L exhibited uniformly reduced intensities as a function of incubation time, and new signals were observed for the 3′-residues of AUG (A345 to A356) (Fig. 1H). Similar NMR spectral changes were observed for an isolated AUG oligo-RNA upon titration with an oligo-U5 fragment (Fig. 1I). The NMR chemical shifts and narrow line widths observed for A345 to A356 indicate that these residues are unstructured and mobile in the dimeric form of the leader ([5′-L]$_2$). No ^{1}H-^{13}C HMQC signals were detected for G328 to G344 of [5′-L]$_2$ because of severe line broadening (discussed below). These findings are consistent with a phylogenetically derived structural model (*10*, *20*), in which the 5′-residues of AUG base pair with U5 and the 3′-residues are disordered (Fig. 1C).

To directly probe for U5:AUG base pairing, we developed an NMR approach that involves replacement of a short stretch of adjacent base pairs by A-U base pairs [long-range probing by adenosine interaction detection (lr-AID)]. The substituting element (ideally [$U_iU_jA_k$]:[$U_lA_mA_n$], but other sequences can suffice) (Fig. 2A) affords an upfield-shifted A_m-C2-^{1}H NMR signal (~6.5 parts per million), enabling direct detection of cross-strand A_k-H2 and -H1′ ^{1}H-^{1}H nuclear Overhauser effects (NOEs), without the need for heteronuclear spectral editing. The HIV-1_{NL4-3} leader naturally contains one [UUA:UAA] element in the TAR hairpin ([U12-A14]:[U45-A47]), and, to preclude signal overlap, A46 was mutated to G [a naturally occurring substitution in 7% of the reported HIV-1 TAR sequences (*31*)] (Fig. 2, B to D). NOE spectroscopy (NOESY) data (*28*) obtained for the lr-AID–modified dimeric 5′-leader ([5′-$L^{lr\text{-}AID\text{-}U5:AUG}$]$_2$, C110 to G112 and G338 to G339 substituted by UUA and AA, respectively) (Fig. 2A) exhibited well-resolved A338-H2 signals with frequencies similar to those observed for an isolated lr-AID–modified U5:AUG oligoribonucleotide (Fig. 2, E and F). Other outlier signals in the NOESY spectrum were unaffected by the lr-AID substitutions. All of the expected A338-H2 inter-adenosine NOEs were observed, including cross-strand NOEs with A112-H1′ and -H2. The A338-H2 T_1 and T_2 ^{1}H NMR relaxation rates (8.7 s and 9.4 ms, respectively) are consistent with restricted rotational motion and indicate that U5:AUG resides within a globular region of the 5′-L structure.

The relationship between U5:AUG formation and dimerization was investigated by means of site-directed mutagenesis. Mutations in AUG designed to stabilize the hairpin and disrupt base pairing with U5 (5′-$L^{AUG\text{-}HP}$) favored the monomer,

[1]Howard Hughes Medical Institute (HHMI) and Department of Chemistry and Biochemistry, University of Maryland Baltimore County (UMBC), 1000 Hilltop Circle, Baltimore, MD 21250, USA. [2]Department of Microbiology and Immunology, University of Michigan Medical School, Ann Arbor, MI 48109–0620, USA.

*Present address: RNA Institute, State University of New York at Albany, 1400 Washington Avenue, Albany, NY 12222, USA.
†These authors contributed equally to this work.
‡To whom correspondence should be sent. E-mail: ateles@umich.edu (A.T.); summers@hhmi.umbc.edu (M.F.S.)

whereas mutations that promote U5:AUG base pairing and destabilize the hairpin ([5′-$L^{U5:AUG}$]$_2$) favored the dimer (fig. S1). Deletion of AUG (5′-$L^{\Delta AUG}$) also favored the monomer (Fig. 3A), whereas incubation of 5′-$L^{\Delta AUG}$ with a 17-nucleotide AUG oligoribonucleotide [G328 to G344 (AUG-17)] promoted dimerization (Fig. 3B). These findings indicate that dimerization is suppressed when AUG exists in a hairpin conformation (AUG^{HP}), that U5:AUG formation promotes dimerization, and that dimerization is induced by intramolecular U5:AUG base pairing rather than intermolecular tethering.

NMR chemical shifts and NOEs associated with A268-H2 in 5′-L, 5′-$L^{\Delta AUG}$, and an isolated DIS oligo-RNA were similar, indicating that the attenuated dimerization activity of the AUG^{HP} form of 5′-L is not due to refolding of the DIS (*32*). Sequence complementarity between U5 and the GC-rich loop of the DIS suggested that dimerization may instead be inhibited by U5:DIS base pairing. Consistent with this hypothesis, mutations in 5′-L designed to enhance U5:DIS base pairing promoted monomer formation (Fig. 3, C and D), whereas mutations to disrupt U5:DIS base pairing induced dimerization of 5′-$L^{\Delta AUG}$ (fig. S2). In addition, NMR data obtained for an lr-AID substituted 5′-$L^{\Delta AUG}$ RNA with 5′-$L^{\Delta AUG}$–like dimerization, and NC binding properties (fig. S4) exhibited cross-strand NOEs and NMR chemical shifts that are consistent with the predicted U5:DIS interface (Fig. 3, E to G).

To determine whether U5:AUG formation influences NC binding, isothermal titration calorimetry (ITC) experiments were performed with 5′-L and mutant 5′-$L^{AUG\text{-}HP}$ and 5′-$L^{U5:AUG}$ RNAs. Under conditions of the ITC experiments, 5′-$L^{AUG\text{-}HP}$ and 5′-$L^{U5:AUG}$ exist predominantly as monomers and dimers, respectively, and native 5′-L exists as a 70:30 monomer:dimer equilibrium mixture (Fig. 4A). All three RNAs gave rise to two-component NC binding isotherms that included an initial exothermic event associated with high-affinity NC binding and a subsequent endothermic event attributed to NC-induced RNA unfolding at high NC:RNA ratios (Fig. 4B and fig. S3) (*33*). Whereas 5′-$L^{AUG\text{-}HP}$ binds 7 ± 1 NC molecules with high affinity (K_d = 87 ± 3 nM),

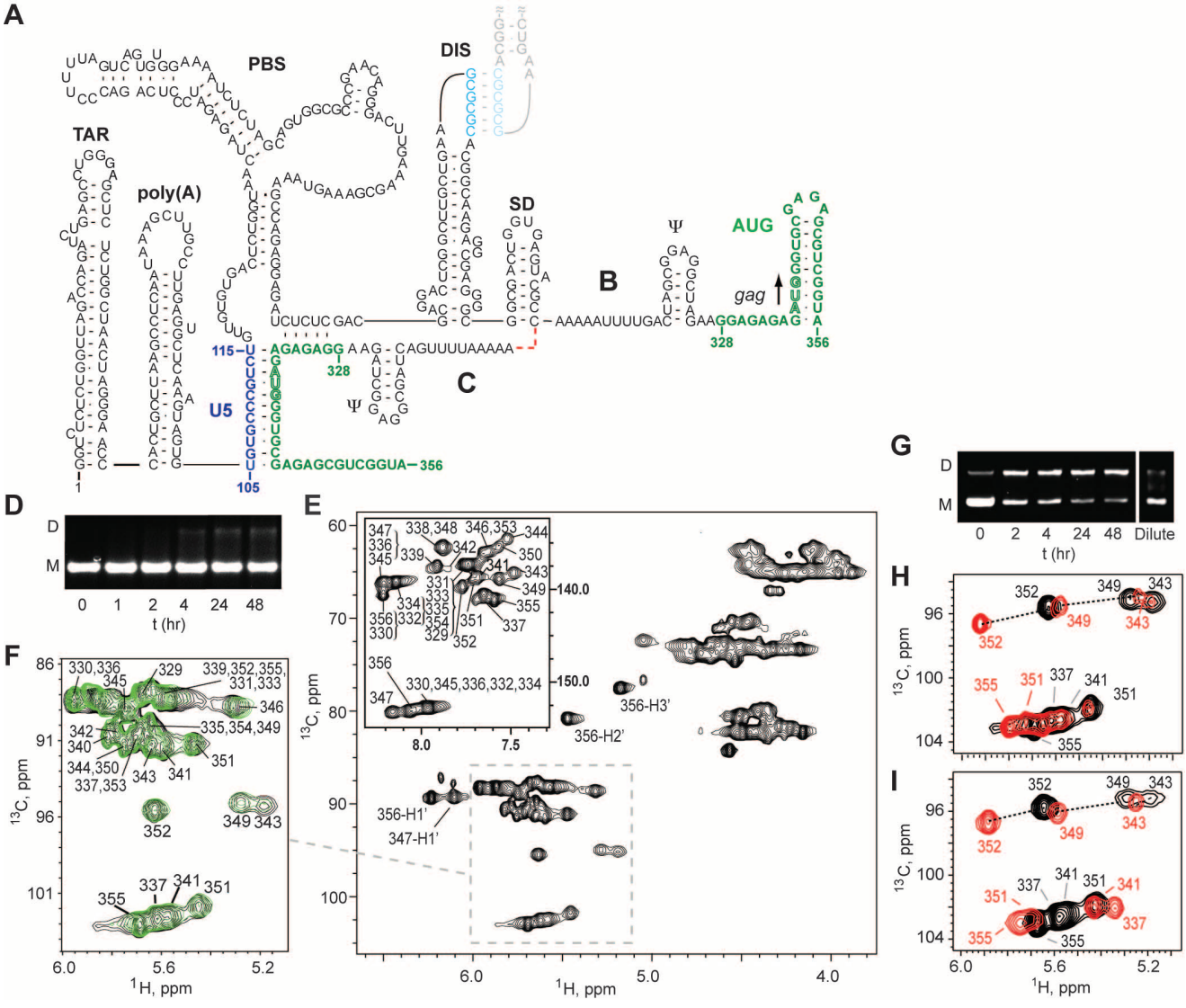

Fig. 1. Structure of the HIV-1 5′-leader. (**A** to **C**) Secondary structure predictions showing AUG (green) in (B) hairpin and (C) U5:AUG conformations. (**D**) 5′-L forms a monomer at low ionic strength [low ion (LI) buffer: 10 mM Tris-HCl, 10 mM NaCl, pH 7.0] ([RNA] = 60 μM). (**E**) 2D ^{1}H-^{13}C HMQC NMR spectrum obtained for 5′-L containing ^{13}C-labeled AUG (5′-L^{AUG*}; LI buffer). (**F**) Overlay of spectra obtained for 5′-L^{AUG*} (gray) and oligo-AUG* hairpin (green). (**G**) 5′-L exists as a reversible monomer-dimer equilibrium in PI buffer ([5′-L] = 30 μM, left). The equilibrium shifts to the monomer upon subsequent dilution (100-fold) in PI buffer. (**H**) ^{1}H-^{13}C HMQC NMR data obtained for 5′-L^{AUG*} in LI buffer (black) and immediately upon dissolution in PI buffer (red). Spectral changes correlate with an equilibrium shift toward the dimer. Residues 349, 351, 352, and 355 are unstructured and detectable, and residues 337 and 341 are rotationally restricted and undetectable, in the $[5'\text{-L}]_2$ dimer. (**I**) Similar spectral changes were observed upon titration of an isolated AUG* hairpin (black) with an unlabeled U5 oligonucleotide, except that all U5:AUG signals were detectable (red).

$[5'\text{-}L^{U5:AUG}]_2$ binds 32 ± 2 NC molecules with high affinity (K_d = 71 ± 3 nM) (Fig. 4B). The ITC profile observed for native 5′-L was similar to that obtained for a 70:30 mixture of $5'\text{-}L^{AUG\text{-}HP}$ and $5'\text{-}L^{U5:AUG}$ (Fig. 4, A and B), validating the use of $5'\text{-}L^{AUG\text{-}HP}$ and $5'\text{-}L^{U5:AUG}$ as models for the native monomer and dimer, respectively. The NC binding and dimerization properties of $5'\text{-}L^{lr\text{-}AID\text{-}U5:AUG}$ and $5'\text{-}L^{lr\text{-}AID\text{-}U5:DIS}$ were similar to those of the $5'\text{-}L^{U5:AUG}$ and $5'\text{-}L^{AUG\text{-}HP}$ controls, respectively (fig. S4), further indicating that the lr-AID substitutions did not alter the structure of the RNA. Substitution of the dimer-promoting GC-rich loop of the DIS hairpin by a GAGA tetraloop prevented dimerization of $5'\text{-}L^{U5:AUG}$ but did not affect its NC-binding properties (fig. S5), indicating that enhanced NC binding by the U5:AUG form of the 5′-leader is due to intramolecular conformational changes associated with U5:AUG base pairing and not to dimerization per se.

The above findings suggested that in vivo RNA packaging should be dependent on U5:AUG formation, and we therefore measured packaging efficiencies of vector RNAs $5'\text{-}L^{AUG\text{-}HP}$ and $5'\text{-}L^{U5:AUG}$ mutations in competition experiments. An HIV-$1_{NL4\text{-}3}$ helper construct that expressed the native 5′-leader and all viral proteins except Env was co-expressed with test vector RNAs with $5'\text{-}L^{AUG\text{-}HP}$ or $5'\text{-}L^{U5:AUG}$ mutations (Fig. 4C). Consistent with the structural and NC binding studies, the $5'\text{-}L^{U5:AUG}$ RNAs were packaged nearly as avidly as the native construct (Fig. 4C, lane 5), whereas the $5'\text{-}L^{AUG\text{-}HP}$ RNAs exhibited severe packaging defects (Fig. 4C, lane 6).

Previously observed packaging defects associated with mutations in AUG (*24*, *34*) can be attributed to defects in U5:AUG–dependent exposure of NC binding sites rather than inhibition of a cis-packaging mechanism (*34*). The inability of helper RNAs to rescue packaging of RNAs with AUG mutations (*24*) is likely due to a defect in U5:AUG–dependent exposure of the DIS because rescue requires DIS-mediated heterodimer formation. The relationship between U5:AUG formation and dimerization also explains why mutations in AUG can lead to the production of virions containing genomes that are sensitive to dissociation by mild denaturants (*25*). Hybrid 5′-leader structures containing both U5:AUG and AUG^{HP} features—predicted from in vivo ribose reactivity measurements (*22*)—were not observed with NMR but can be explained by the presence of the AUG^{HP}/U5:AUG equilibrium. Elevated U5 nucleotide reactivities observed by traditional chemical probing, which are incompatible with an exclusive U5:AUG structure (*21*), may also be explained by the observed AUG^{HP}/U5:AUG equilibrium. The finding that the *gag* start codon is exposed in a mobile hairpin in the monomeric leader and sequestered in the dimer is consistent with observations that dimerization attenuates both the chemical reactivity of the *gag* start codon and the in vitro translational activity of the genome (*16*).

We have developed an approach that extends the size of RNAs that can be structurally probed by NMR to ~230 kD. The lr-AID method avoids NMR relaxation problems associated with heteronuclear editing, probes interactions over a narrow distance range (≲5 Å), provides both chemical shift and distance information for structural analysis, and is readily implemented by using standard two-dimensional (2D) NMR experiments and conservative base-pair mutagenesis. Our findings support a translation/packaging RNA structural switch mechanism, in which the dimer-promoting GC-rich loop of the DIS hairpin is sequestered by base pairing with U5 in the AUG^{HP} form of the 5′-leader and is displaced by AUG upon U5:AUG formation (Fig. 4D).

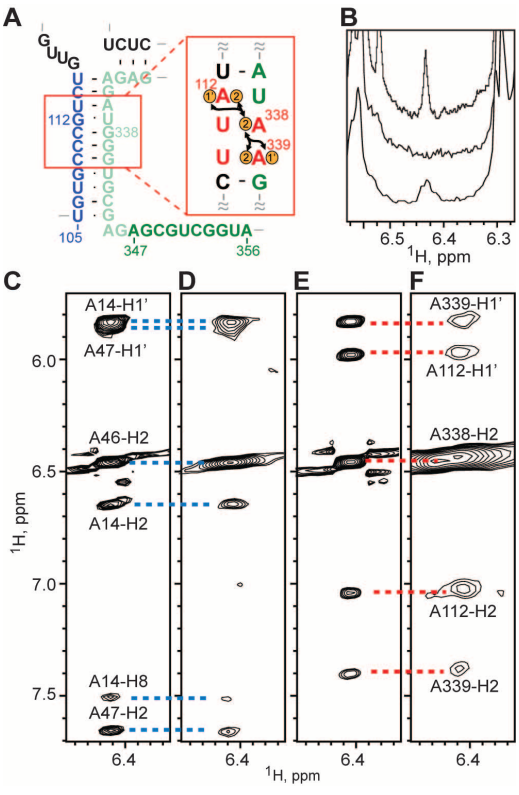

Fig. 2. AUG base pairs with U5 in the dimer. (**A**) lr-AID mutations (red) designed to probe for predicted U5:AUG base pairing. Black arrows denote ^{1}H-^{1}H NOEs. (**B**) Portions of 1D ^{1}H NMR spectra showing (top) the TAR A46-H2 signal of native $[5'\text{-}L]_2$; (middle) A46G substitution ($[5'\text{-}L^{A46G}]_2$) eliminates the TAR A46-H2 signal; and (bottom) A338-H2 signal observed for lr-AID substituted $[5'\text{-}L^{A46G}]_2$. (**C** and **D**) Similarities in NOE spectra observed for A46-H2 of (C) an isolated TAR oligonucleotide and (D) native $[5'\text{-}L]_2$. (**E** and **F**) Similar A338-H2 NOEs observed for (E) an isolated lr-AID U5:AUG oligonucleotide and (F) lr-AID substituted $[5'\text{-}L^{A46G}]_2$.

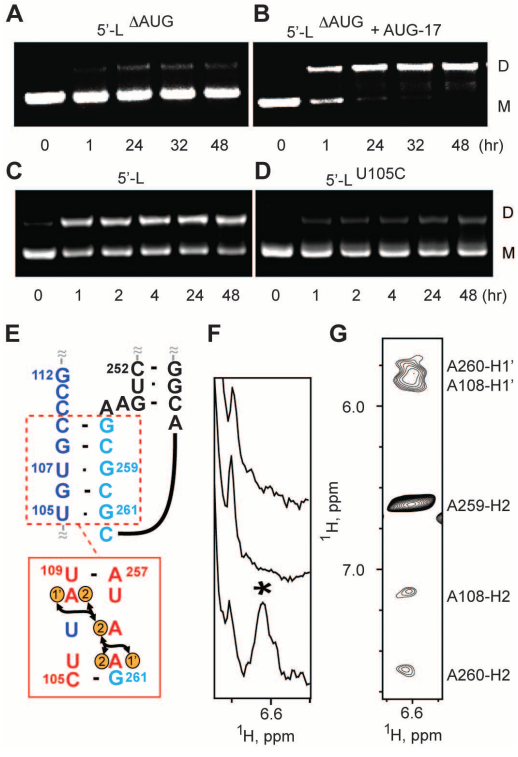

Fig. 3. U5:AUG formation promotes dimerization. (**A**) $5'\text{-}L^{\Delta AUG}$ (1 μM) forms a stable monomer. (**B**) Addition of AUG-17 (10-fold molar excess) promotes dimerization of $5'\text{-}L^{\Delta AUG}$. (**C** and **D**) Substitutions that enhance U5:DIS interactions favor the monomer. (**E**) Proposed U5:DIS base pairing and lr-AID sequences used for structural probing. (**F**) The A259-H2 signal is only observed when U5 and DIS both contain lr-AID substitutions. (Top) $5'\text{-}L^{\Delta AUG,A46G}$. (Middle) $5'\text{-}L^{\Delta AUG,A46G}$ containing the lr-AID substitution in the DIS loop only. (Bottom) $5'\text{-}L^{\Delta AUG,A46G}$ containing lr-AID substitution in both DIS and U5. (**G**) 2D NOE data for A259-H2 in lr-AID–substituted $5'\text{-}L^{\Delta AUG,A46G}$, assigned from the corresponding U5:DIS oligonucleotide control spectrum.

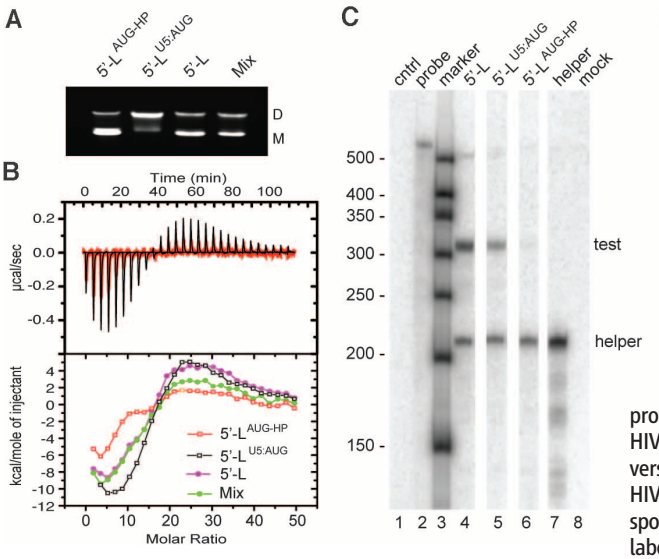

Fig. 4. U5:AUG formation promotes NC binding and packaging. (**A**) 5′-L^{AUG-HP} and 5′-L$^{U5:AUG}$ form predominantly monomers and dimers, respectively, and native 5′-L adopts a 70:30 monomer:dimer equilibrium (PI buffer; [RNA] = 0.8 μM). Mix, 70:30 mixture of 5′-L^{AUG-HP} and 5′-L$^{U5:AUG}$. (**B**) ITC NC titration data for samples shown in (A). (**C**) Packaging of native HIV-1$_{NL4-3}$ 5′-L, 5′-L$^{U5:AUG}$, and 5′-L^{AUG-HP} RNAs under competition conditions [assayed by means of ribonuclease protection (*28*)]. Lanes 2 to 8: 2, undigested probe; 3, RNA size standards; 4, native HIV-1$_{NL4-3}$ helper versus native HIV-1$_{NL4-3}$ test vector RNAs; 5, native HIV-1$_{NL4-3}$ helper versus 5′-L$^{U5:AUG}$ test vector; 6, native HIV-1$_{NL4-3}$ helper versus 5′-L^{AUG-HP} test vector; 7, HIV-1$_{NL4-3}$ helper expressed without test RNA; 8, mock transfected-cells. Bands corresponding to native HIV-1$_{NL4-3}$ helper RNA (helper) and copackaged test RNAs (test) are labeled. (**D**) Nucleotide displacement mechanism regulates dimeric genome packaging.

Conformational changes associated with U5:AUG base pairing simultaneously sequester the *gag* start codon and expose the DIS and high-affinity NC binding sites, attenuating translation and promoting the packaging of a dimeric genome.

References and Notes

1. J. M. Coffin, S. H. Hughes, H. E. Varmus, *Retroviruses* (Cold Spring Harbor Laboratory Press, Plainview, NY, 1997).
2. A. M. Lever, *Adv. Pharmacol.* **55**, 1 (2007).
3. A. Onafuwa-Nuga, A. Telesnitsky, *Microbiol. Mol. Biol. Rev.* **73**, 451 (2009).
4. E. Poole, P. Strappe, H. P. Mok, R. Hicks, A. M. Lever, *Traffic* **6**, 741 (2005).
5. M. D. Moore *et al.*, *PLoS Pathog.* **5**, e1000627 (2009).
6. S. B. Kutluay, P. D. Bieniasz, *PLoS Pathog.* **6**, e1001200 (2010).
7. J.-C. Paillart, M. Shehu-Xhilaga, R. Marquet, J. Mak, *Nat. Rev. Microbiol.* **2**, 461 (2004).
8. N. Jouvenet, S. M. Simon, P. D. Bieniasz, *Proc. Natl. Acad. Sci. U.S.A.* **106**, 19114 (2009).
9. G. Miele, A. Mouland, G. P. Harrison, E. Cohen, A. M. Lever, *J. Virol.* **70**, 944 (1996).
10. T. E. M. Abbink, B. Berkhout, *J. Biol. Chem.* **278**, 11601 (2003).
11. R. S. Russell, C. Liang, M. A. Wainberg, *Retrovirology* **1**, 23 (2004).
12. J. Greatorex, *Retrovirology* **1**, 23 (2004).
13. V. D'Souza, M. F. Summers, *Nat. Rev. Microbiol.* **3**, 643 (2005).
14. K. Lu, X. Heng, M. F. Summers, *J. Mol. Biol.* **410**, 609 (2011).
15. G. P. Harrison, A. M. L. Lever, *J. Virol.* **66**, 4144 (1992).
16. F. Baudin *et al.*, *J. Mol. Biol.* **229**, 382 (1993).
17. J. Clever, C. Sassetti, T. G. Parslow, *J. Virol.* **69**, 2101 (1995).
18. M. S. McBride, A. T. Panganiban, *J. Virol.* **70**, 2963 (1996).
19. J. L. Clever, D. Miranda Jr., T. G. Parslow, *J. Virol.* **76**, 12381 (2002).
20. C. K. Damgaard, E. S. Andersen, B. Knudsen, J. Gorodkin, J. Kjems, *J. Mol. Biol.* **336**, 369 (2004).
21. J. C. Paillart *et al.*, *J. Biol. Chem.* **279**, 48397 (2004).
22. K. A. Wilkinson *et al.*, *PLoS Biol.* **6**, e96 (2008).
23. J. M. Watts *et al.*, *Nature* **460**, 711 (2009).
24. O. Nikolaitchik, T. D. Rhodes, D. Ott, W.-S. Hu, *J. Virol.* **80**, 4691 (2006).
25. R. Song, J. Kafaie, M. Laughrea, *Biochemistry* **47**, 3283 (2008).
26. F. H.-T. Allain, G. Varani, *J. Mol. Biol.* **267**, 338 (1997).
27. B. S. Tolbert *et al.*, *J. Biomol. NMR* **47**, 205 (2010).
28. Materials and methods are available as supporting material on *Science* Online.
29. D. J. Kerwood, M. J. Cavaluzzi, P. N. Borer, *Biochemistry* **40**, 14518 (2001).
30. E. T. Yu, A. Hawkins, J. Eaton, D. Fabris, *Proc. Natl. Acad. Sci. U.S.A.* **105**, 12248 (2008).
31. The HIV Sequence Database; available at www.hiv.lanl.gov/content/sequence/HIV/mainpage.html (2011).
32. H. Huthoff, B. Berkhout, *RNA* **7**, 143 (2001).
33. M. F. Summers *et al.*, *Protein Sci.* **1**, 563 (1992).
34. D. T. Poon, E. N. Chertova, D. E. Ott, *Virology* **293**, 368 (2002).

Acknowledgments: This research was supported by a grant (R01 GM42561) from the National Institute of General Medical Sciences (NIGMS). L.G. was supported by a NIGMS grant for maximizing doctoral diversity (R25 MBRS-IMSD GM55036). B.D., K.E., S.J., G.K., and S.B. were supported by a NIGMS grant for enhancing minority access to research careers (MARC U*STAR 2T34 GM008663). B.D., G.K., and S.B. were supported by a HHMI undergraduate education grant. We thank S. R. King (Michigan) and HHMI staff (UMBC) for technical assistance.

Supporting Online Material

www.sciencemag.org/cgi/content/full/334/6053/242/DC1
Materials and Methods
Figs. S1 to S5
References (*35*–*48*)

28 June 2011; accepted 9 September 2011
10.1126/science.1210460

Successful Transmission of a Retrovirus Depends on the Commensal Microbiota

Melissa Kane,[1] Laure K. Case,[1]* Karyl Kopaskie,[1] Alena Kozlova,[1] Cameron MacDearmid,[1] Alexander V. Chervonsky,[2]† Tatyana V. Golovkina[1]†‡

To establish chronic infections, viruses must develop strategies to evade the host's immune responses. Many retroviruses, including mouse mammary tumor virus (MMTV), are transmitted most efficiently through mucosal surfaces rich in microbiota. We found that MMTV, when ingested by newborn mice, stimulates a state of unresponsiveness toward viral antigens. This process required the intestinal microbiota, as antibiotic-treated mice or germ-free mice did not transmit infectious virus to their offspring. MMTV-bound bacterial lipopolysaccharide triggered Toll-like receptor 4 and subsequent interleukin-6 (IL-6)–dependent induction of the inhibitory cytokine IL-10. Thus, MMTV has evolved to rely on the interaction with the microbiota to induce an immune evasion pathway. Together, these findings reveal the fundamental importance of commensal microbiota in viral infections.

Successful pathogens have developed means to counteract the immune system or even to use established immune mechanisms to their own benefit. Retroviruses, including mouse mammary tumor virus (MMTV), are detected by at least one Toll-like receptor (TLR7), and detection is dependent on the adaptor molecule that signals downstream of most TLRs, expressed by myeloid differentiation primary response gene 88 (MyD88) (*1*–*3*). Retroviruses employ various mechanisms of immune evasion (*4*, *5*), however, and can destroy the immune system (e.g., immunodeficiency viruses of various species) or subvert it (*5*, *6*) to enable successful transmission. Establishment of a state of immunological tolerance to viral proteins in infected animals should also support virus spread. To test whether animals infected with the orally transmitted MMTV were tolerant to MMTV antigens, we immunized

[1]Department of Microbiology, The University of Chicago, Chicago, IL 60637, USA. [2]Department of Pathology, The University of Chicago, Chicago, IL 60637, USA.

*Present address: The University of Vermont, Given C249, 89 Beaumont Avenue, Burlington, VT 05405, USA.
†These authors contributed equally to this work.
‡To whom correspondence should be addressed. E-mail: tgolovki@bsd.uchicago.edu

NMR Detection of Structures in the HIV-1 5#-Leader RNA That Regulate Genome Packaging

Kun Lu, Xiao Heng, Lianko Garyu, Sarah Monti, Eric L. Garcia, Siarhei Kharytonchyk, Bilguujin Dorjsuren, Gowry Kulandaivel, Simonne Jones, Atheeth Hiremath, Sai Sachin Divakaruni, Courtney LaCotti, Shawn Barton, Daniel Tummillo, Azra Hosic, Kedy Edme, Sara Albrecht, Alice Telesnitsky, and Michael F. Summers

Science **334** (6053), . DOI: 10.1126/science.1210460